

Brain MR Image Denoising for Rician Noise Using Intrinsic Geometrical Information

Hamit Soyel, Kamil Yurtkan, Hasan Demirel and Peter W. McOwan

Abstract A new image denoising algorithm based on nonsubsampling contourlet transform is presented. Magnetic Resonance (MR) images corrupted by Rician noise are transformed into multi-scale and multi-directional contour information, where a nonlinear mapping function is used to modify the contour coefficients at each level. The denoising is achieved by improving edge sharpness and inhibiting the background noise. Experiments show the proposed algorithm preserves the intrinsic geometrical information of the noised MR image and can be effectively applied to T1-, T2-, and PD-weighted MR images without any parameter tuning under diverse noise levels.

1 Introduction

By analysing magnetic resonance (MR) images of the brain, surgeons can make an appropriate decision for diagnosing many neurological diseases, such as Parkinsons disease, Alzheimers disease, brain tumors, and stroke. However, MR images are affected by several artifacts and noise sources. One of them is the random fluctuation of the MR signal which is mainly due to thermal noise. Such a noise seriously degrades the acquisition of any quantitative measurements from the MR images, such as registration, segmentation, classification, and visualization. To obtain reliable

H. Soyel (✉) · P.W. McOwan
Queen Mary University of London, London, UK
e-mail: h.soyel@qmul.ac.uk

P.W. McOwan
e-mail: p.mcowan@qmul.ac.uk

K. Yurtkan
Cyprus International University, Lefkoşa, Mersin Turkey
e-mail: kyurtkan@ciu.edu.tr

H. Demirel
Eastern Mediterranean University, Gazimağusa, Mersin Turkey
e-mail: hasan.demirel@emu.edu.tr

analysis results, denoising MR image is vital before further analysis steps can be conducted. MR images are computed from both real and imaginary images, which are assumed to contain Gaussian distribution noises with zero means. Thus, noise is image dependent, which follows a Rician distribution, and makes removing noises difficult [12].

Postprocessing filtering techniques have the advantage of not increasing the acquisition time and, hence have been extensively used in MR image denoising. Most denoising methods are based on the signal averaging principle by using the spatial pattern redundancy in the image. However, there are other filtering techniques that use other statistical estimates such as the Median [10], Gaussian [1] and Anisotropic Diffusion [16] that have received considerable attention due to their simplicity. Although these denoising methods can significantly remove noise, they tend to cause blurring and erase small features if there are high peaks in the histogram, often resulting a mask effect in uniform regions and other artifacts in the output image.

One way to approaching this problem is to use multi-scale image decomposition, that is, processing images in each scale independently and recombining each processed image to obtain the final image. Advances in wavelet theory combined with multi-scale analysis applied to image contrast enhancement can achieve promising results. The decomposition of images into different frequency ranges permits the isolation of the frequency components introduced by intrinsic deformations or extrinsic factors in certain subbands [18].

In [13], the undecimated wavelet transform is employed to provide effective representation of the noisy coefficients information. However, the 2D wavelet transform used is a separable extension of the 1D wavelet transform, which does not work well in capturing the geometry of image edges [14].

We propose a new image enhancement method based on the nonsubsampled contourlet transform (NSCT) [6]. The proposed algorithm enhances the MR image while amplifying weak edges and suppressing noise by modifying the NSCT coefficients using a nonlinear mapping function in each directional subband.

The rest of this paper is organized as follows. In Sect. 2, we explain the intrinsic geometrical information based methodology for image denoising. A variety of experimental results are presented in Sect. 3. Finally, the conclusions are given in Sect. 4.

2 Methodology

Existing image-denoising methods amplify noise when they amplify weak edges since they cannot distinguish noise from weak edges. In the frequency domain, both weak edges and noise produce low-magnitude coefficients. Since weak edges are geometric structures and noise is not, we can use the NSCT to distinguish them [17].

2.1 Nonsampled Countourlet Transform

In [7], Do and Vetterli proposed the contourlet transform (CT), which is a multiscale directional representation constructed in the discrete grid by combining the Laplacian pyramid and the directional filter bank. Due to its directionality and anisotropy CT can represent curve more sparsely. NSCT, based on the theory of CT, is a kind of multi-scale, multi-directional computation framework of discrete images. The main difference lies in that, in the course of decomposition and reconstruction, traditional upsamplers and downsamplers in CT do not exist in NSCT any more, so that the NSCT is a fully multi-scale, multi-directional, good time-frequency property and shift invariant expansion.

NSCT falls into two phases, including nonsampled pyramid (NSP) and non-sampled directional filter bank (NSDFB). The former phase ensures the multi-scale property by using two-channel nonsampled filter bank, and a low-pass image with a band-pass one can be produced at each NSP decomposition stage. The subsequent NSP decomposition stages are carried out to decompose the low-pass component available iteratively to capture the singularities in the image. As a result, NSP can result in $k + 1$ subband images including one low-pass image and k band-pass images, whose sizes are all the same as that of the source image, where k denotes the number of decomposition stages. Figure 1 gives the NSP decomposition with $k = 3$ stages with a 2-D low-pass filter is represented by its z -transform $H_0(z)$ where $z = [z_1, z_2]^T$ and $H_1(z) = 1 - H_0(z)$. The filters for subsequent stages are obtained by upsampling the filters of the first stage. This gives the multi-scale property without the need for additional filter design. The NSDFB, constructed by combining the directional fan filter banks devised by Bamberger and Smith [2], is two-channel nonsampled filter banks. NSDFB allows the direction decomposition with l stages in band-pass images from NSP at each scale and produces $2l$ directional subband images which have the same size as the source image. Thus, the NSDFB endows the NSCT with the multi-direction property and we can benefit a lot from

Fig. 1 Three-stage NSP decomposition

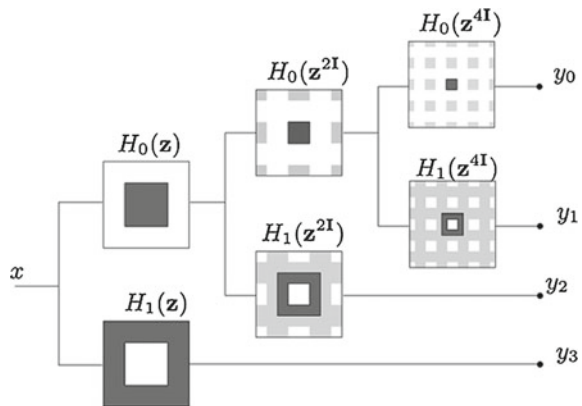
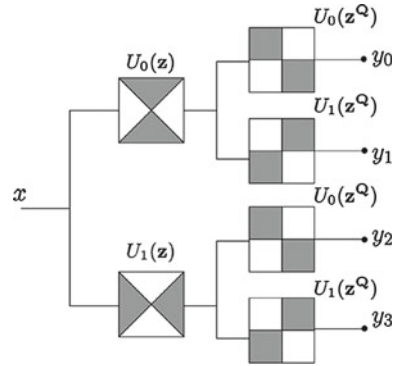


Fig. 2 Four-channel nonsampled DFB



the NSDFB because it provides us with more precise directional detail information. A four-channel NSDFB, constructed with two-channel fan filter banks and parallelogram filters without downsamplers and upsamplers, is illustrated in Fig. 2. Note that in the second level, the upsampled fan filters $U_i(z^Q), i = 0, 1$ have checker-board frequency support, and when combined with the filters in the first level give the four directional frequency decomposition. We use the ‘maxat’ filters and ‘dmaxat7’ filters for NSP and NSDFB, respectively. The concrete filter banks construction methods and more NSCT details can be found in [6].

2.2 Proposed Image Denoising Using Intrinsic Geometrical Information

NSCT differs from other multi-scale analysis methods in that contourlet transform allows for different and flexible number of directions at each scale. According the direction information contours are obtained by directional filter bank concatenated the neighbouring singular points into local contours in the frequency domain. By combination of NSP and NSDFB, NSCT is constructed as a fully shift invariant, multi-scale, and multi-direction expansion that has better directional frequency localization and a fast implementation. It is worth noting that shift invariance is very important. Being shift invariant, each pixel of the transform subbands corresponds to that of the original image in the same spatial location. Therefore, we gather the geometrical information pixel by pixel from the NSCT coefficients. All directional contour subbands can be expressed as:

$$\{C_{m,d}\}, m = 1, 2, \dots, k, d = 1, 2, \dots, l_m, k \in (1, 2, \dots, N), l_m = 2^N. \tag{1}$$

where m and d are the scale and direction of the decomposition respectively, k is the number of contour decomposition scale, l_m is the number of contour decomposition directions of m th scale and $\{C_{m,d}\}$ is the coefficient at the d th directional subband of the m th scale. We observe that in the NSCT domain, the Rician noise corresponds to those pixels with small magnitude coefficients in all directional subbands at a specific pyramidal level. Based on this observation, we can classify pixels into two categories by analysing the distribution of their coefficients in different subbands. One simple way is to compute the mean (denoted by mean) and the maximum (denoted by max) magnitude of the coefficients for each pixel across directional subbands, and then classify it by:

$$\text{pixel} = \begin{cases} \text{noise,} & \text{if}((\text{mean} < \alpha\sigma\gamma) \text{ and } (\text{max} < \alpha\sigma\gamma)) \\ \text{edge,} & \text{otherwise} \end{cases} \quad (2)$$

where α is the amplifying gain of the subbands at a specific pyramidal level (3), σ is the noise variance of the input MR image and γ is the noise standard deviation of the subbands at a specific pyramidal level.

$$\alpha = \frac{\log\left(\frac{\text{mean}(|C_{m,d}|)}{\text{max}(|C_{m,d}|)}\right)}{\log\left(\sin\left(\frac{\pi}{2} \frac{\text{mean}(|C_{m,d}|)}{\text{max}(|C_{m,d}|)}\right)\right)} \quad (3)$$

We first estimate the noise variance of the input MR image, $\hat{\sigma}$, with the robust median operator defined in [4] and then compute the noise variance of each subband, $\hat{\gamma}$, by using [18]. The core requirement for image denoising by multi-scale transforms is to suppressing noise while amplifying weak edges. To this end we modify the NSCT coefficients, $\tilde{C}_{m,d}$, by a nonlinear mapping function in each scale and direction where $m > 1$:

$$\tilde{C}_{m,d} = \begin{cases} \left(\frac{\text{max}(|C_{m,d}|)}{\text{sgn}(C_{m,d})}\right) \sin\left(\frac{\pi}{2} \sin\left(\frac{\pi}{2} \frac{|C_{m,d}|}{\text{max}(|C_{m,d}|)}\right)^\alpha\right)^{\sqrt{\alpha}}, & \text{edge} \\ 0, & \text{noise.} \end{cases} \quad (4)$$

We summarize our denoising method in the following algorithm.

1. Compute the NSCT of the input MR image for k levels according to (1).
2. Estimate the noise standard deviation ($\hat{\sigma}$) of the input image.

3. For each level of the pyramid where $m > 1$:
 - a. Estimate the noise variance ($\hat{\gamma}$).
 - b. At each pixel location, compute the mean and the maximum magnitude of the corresponding coefficients in all directional subbands at this level, and classify each pixel according to (2) and (3) into “edges” or “noise”.
 - c. For each directional subband, use the nonlinear mapping function given in (4) to modify the NSCT coefficients according to the classification.
4. Reconstruct the denoised MR image from the modified NSCT coefficients.

3 Experimental Results

We have compared the performance of our proposed image denoising using intrinsic geometrical information with two state-of-the-art denoising algorithms, the non-local mean (NLM) algorithm [3] and a modern wavelet-based denoising algorithm (SURELET) [11] using the 3D-simulated MR images downloaded from the

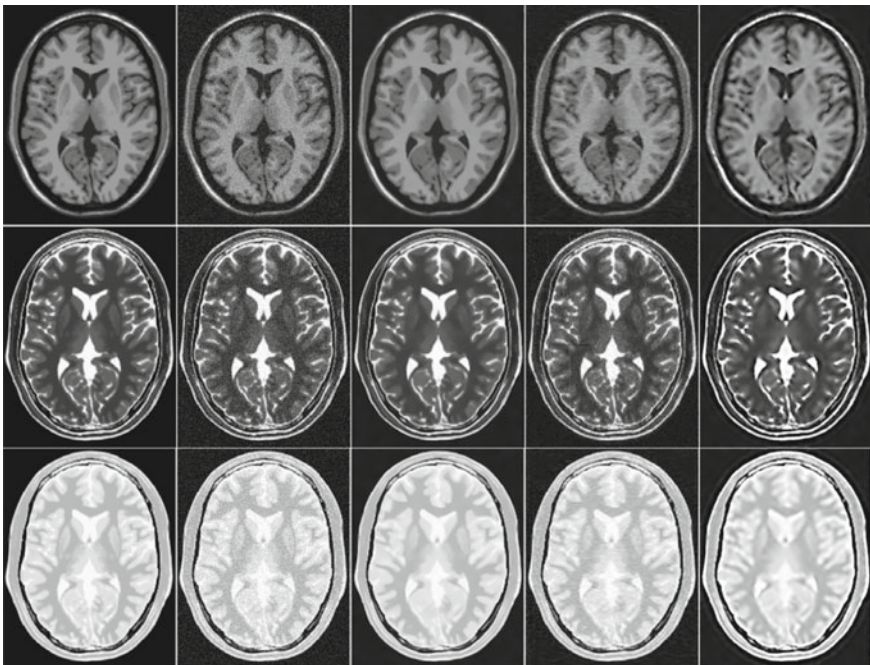


Fig. 3 Visual quality comparison: *Top row*; from *left to right*: **a** Ground truth T1-weighted image. **b** Ground truth corrupted with Rician noise of 13%. Denoised with **c** NLM, **d** SURELET and **e** the proposed method. *Middle row*; and *bottom row*: same results for a simulated T2- and PD-weighted images

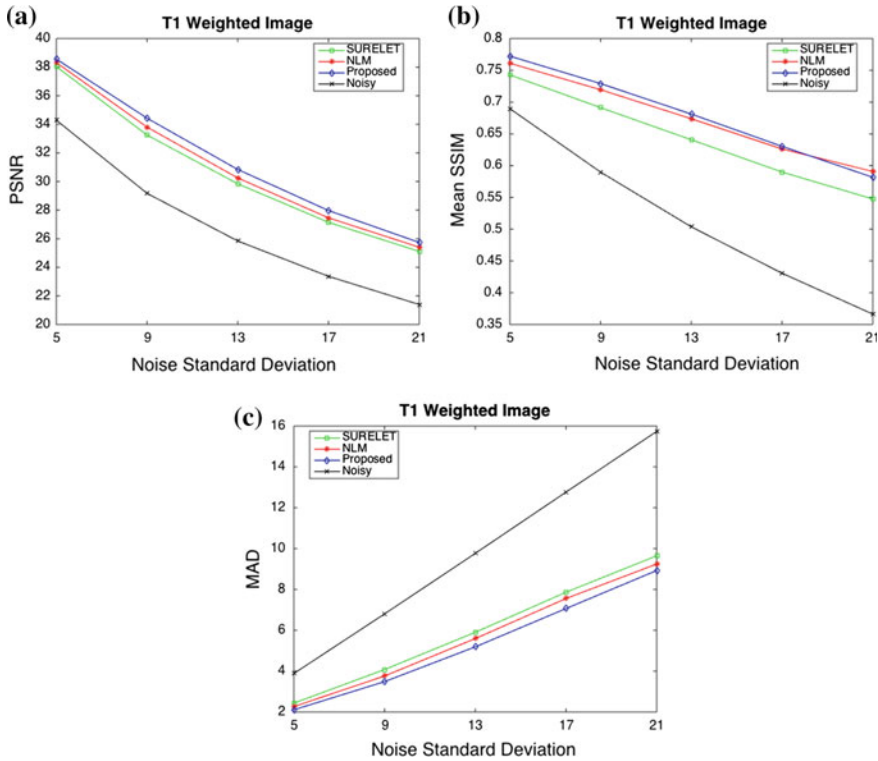


Fig. 4 Quantitative comparison of the proposed NSTC based denoising method with NLM and SURELET methods based on **a** PSNR, **b** SSIM and **c** MAD for simulated T1 images corrupted with Rician noise varying from 5 to 21

BrainWeb database [5]. The simulated T1-, T2-, and PD-weighted synthetic noise-free MR images are downloaded where the size of each image is $181 \times 217 \times 181$ and the intensity is 256 bins.

Visual quality comparison of the MR images denoised with the NLM, the SURELET and the proposed method was conducted on the simulated T1-, T2-, and PD-weighted synthetic noise-free MR images after corrupting the images by Rician noise [8] with 13%. It can be observed from Fig. 3 that the images denoised with the proposed method are more closer to the ground truth than the images denoised with the other approaches.

For a quantitative analysis, MR images were degraded with Rician noise for a wide range of noise levels and the denoising efficiency of the algorithms was evaluated based on the Peak Signal to Noise Ratio (PSNR) [9], the mean Structural Similarity Index Matrix (SSIM) [19] and the Mean Absolute Difference (MAD) [15]. A higher

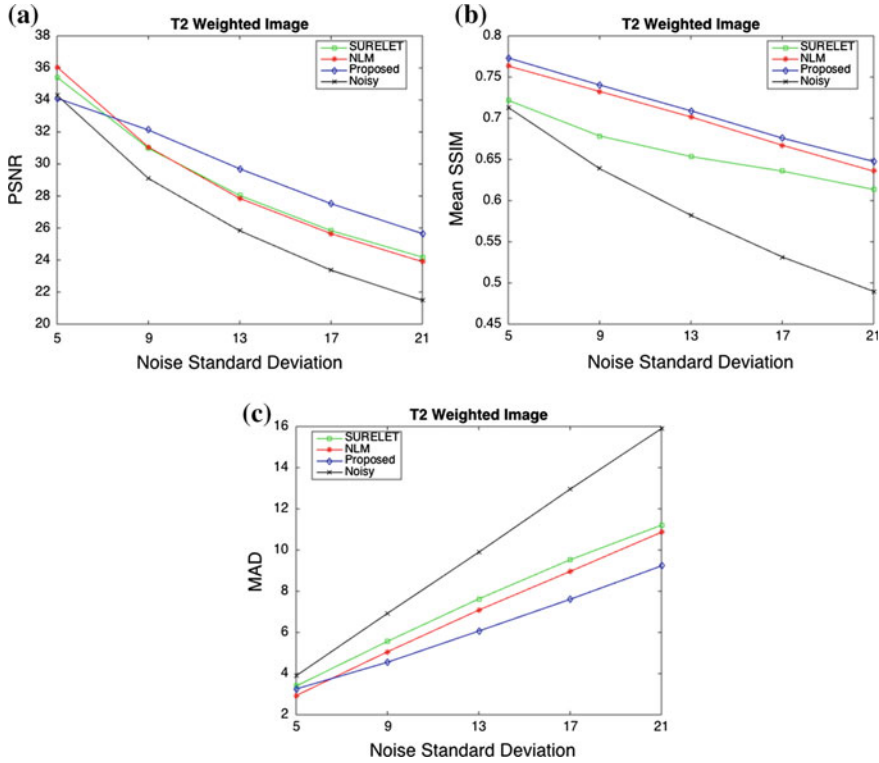


Fig. 5 Quantitative comparison of the proposed NSTC based denoising method with NLM and SURELET methods based on **a** PSNR, **b** SSIM and **c** MAD for simulated T2 images corrupted with Rician noise varying from 5 to 21

PSNR, MSSIM and a lower MAD correspond to a higher performance. Figures 4, 5 and 6 show the quantitative analysis of the denoising methods in terms of PSNR, mean SSIM and MAD. It can be observed from the plots that the proposed method performs better than the NLM and SURELET based on the quality metrics used for the evaluation. Furthermore, proposed methodology does not require any parameter selection and on a PC with 2.5 GHz Intel Core i5 CPU and 8 GB RAM, NSCT costs on average of 5.23 s to decompose a 181×217 MR image into directional subbands and to reconstruct denoised MR image using Matlab¹ hence, can be easily applied for a clinical application.

¹The nonsubsamped contourlet toolbox used in this paper can be downloaded at <http://www.mathworks.com/matlabcentral/fileexchange/10049-nonsubsamped-contourlet-toolbox>.

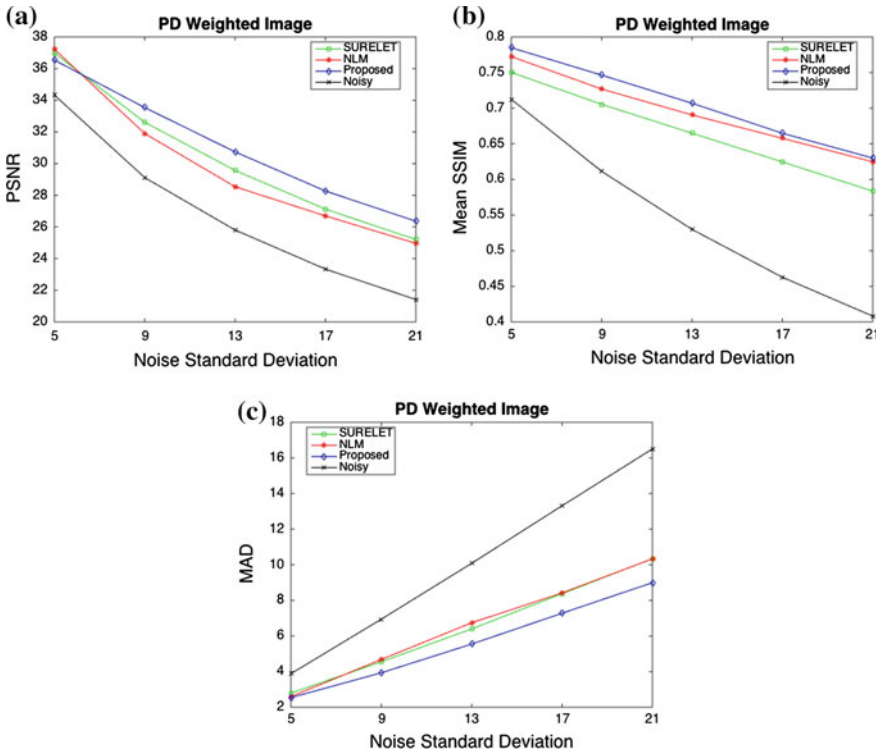


Fig. 6 Quantitative comparison of the proposed NSTC based denoising method with NLM and SURELET methods based on a PSNR, b SSIM and c MAD for simulated PD images corrupted with Rician noise varying from 5 to 21

4 Conclusion

We have proposed a novel multi-scale image denoising algorithm to remove Rician noise from MR images based on the NSCT. We have shown that the new algorithm can sufficiently remove Rician noise, while simultaneously preserving edges and fine structures in a given noisy MR image. Experimental results on the BrainWeb database verified that the intrinsic geometrical information extracted from directional contour coefficients is quite efficient, speedy and can be effectively applied to T1-, T2-, and PD-weighted MR images without any parameter tuning under diverse noise levels.

References

1. Ashburner, J., Friston, K.J.: Voxel-based morphometry—the methods. *NeuroImage* **11**(6), 805–821 (2000)
2. Bamberg, R.H., Smith, M.J.T.: A filter bank for the directional decomposition of images: theory and design. *IEEE Trans. Sig. Process.* **40**(4), 882–893 (1992)
3. Buades, A., Coll, B., Morel, J.M.: A non-local algorithm for image denoising. *Computer Vision and Pattern Recognition. CVPR 2005. IEEE Computer Society Conference on* 2, 60–65 (2005)
4. Chang, S., Yu, B., Vetterli, M.: Spatially adaptive wavelet thresholding with context modeling for image denoising. *IEEE Trans. Image Process.* **9**(9), 1522–1531 (2000)
5. Cocosco, C.A., Kollokian, V., Kwan, Evans, A.C.: BrainWeb: Online interface to a 3D MRI simulated brain database. *NeuroImage* **5**(4) (1997)
6. da Cunha, A., Zhou, J., Do, M.: The nonsubsampling contourlet transform: Theory, design, and applications. *IEEE Trans. Image Process.* **15**(10), 3089–3101 (2006)
7. Do, M., Vetterli, M.: The contourlet transform: An efficient directional multiresolution image representation. *IEEE Trans. Image Process.* **14**(12), 2091–2106 (2005)
8. Gudbjartsson, H., Patz, S.: The Rician distribution of noisy MRI data. *Magn. Reson. Med.* **34**, 910–914 (1995)
9. Huynh-Thu, Q., Ghanbari, M.: Scope of validity of PSNR in image/video quality assessment. *Electron. Lett.* **44**(13), 800–801 (2008)
10. Livin, M., Luthon, F., Keeve, E.: Entropic estimation of noise for medical volume restoration. *Proceedings of the 16th International Conference on Pattern Recognition*, **16**(3), 871–874 (2002)
11. Luisier, F., Blu, T., Unser, M.: A new SURE approach to image denoising: Interscale orthonormal wavelet thresholding. *IEEE Trans. Image Process.* **16**(3), 593–606 (2007)
12. Manjri, J.V., Carbonell-Caballero, J., Lull, J.J., Garcia-Mart, G., Mart-Bonmat, L., Robles, M.: MRI denoising using non-local means. *Med. Image Anal.* **12**(4), 514–523 (2008)
13. Pizurica, A., Philips, W., Lemahieu, I., Acheroy, M.: A versatile wavelet domain noise filtration technique for medical imaging. *IEEE Trans. Med. Imaging* **22**(3), 323–331 (2003)
14. Po, D.Y., Do, M.: Directional multiscale modeling of images using the contourlet transform. *IEEE Trans. Image Process.* **15**(6), 1610–1620 (2006)
15. Rajan, J., Jeurissen, B., Verhoye, M., Audekerke, J.V., Sijbers, J.: Maximum likelihood estimation-based denoising of magnetic resonance images using restricted local neighborhoods. *Phys. Med. Biol.* **56**(16), 5221 (2011)
16. Samsonov, A., Johnson, C.: Noise-adaptive nonlinear diffusion filtering of MR images with spatially varying noise levels. *Magn. Reson. Med.* **52**(4), 798–806 (2004)
17. Soyel, H., McOwan, P.: Automatic image enhancement using intrinsic geometrical information. *Electron. Lett.* **48**(15), 917–919 (2012)
18. Starck, J.L., Candes, E., Donoho, D.: The curvelet transform for image denoising. *IEEE Trans. Image Process.* **11**(6), 670–684 (2002)
19. Wang, Z., Bovik, A., Sheikh, H., Simoncelli, E.: Image quality assessment: from error visibility to structural similarity. *IEEE Trans. Image Process.* **13**(4), 600–612 (2004)